Gene Therapy (2005) 12, 1023–1032

www.nature.com/gt

RESEARCH ARTICLE

Quantitative comparison of polyethylenimine formulations and adenoviral vectors in terms of intracellular gene delivery processes

CM Varga[1,4,5], NC Tedford[1,4,5], M Thomas[2,4], AM Klibanov[1,2,4], LG Griffith[1,3,4] and DA Lauffenburger[1,4]
[1]Biological Engineering Division, Massachusetts Institute of Technology, Cambridge, MA, USA; [2]Department of Chemistry, Massachusetts Institute of Technology, Cambridge, MA, USA; [3]Department of Mechanical Engineering, Massachusetts Institute of Technology, Cambridge, MA, USA; and [4]Biotechnology Process Engineering Center, Massachusetts Institute of Technology, Cambridge, MA, USA

An objective of designing molecular vehicles exhibiting virus-like transgene delivery capabilities but with low toxicity and immunogenicity continues to drive synthetic vector development. As no single step within the gene delivery pathway represents the critical limiting barrier for all vector types under all circumstances, improvements in synthetic vehicle design may be aided by quantitative analysis of the contributions of each step to the overall delivery process. To our knowledge, however, synthetic and viral gene delivery methods have not yet been explicitly compared in terms of these delivery pathway steps in a quantitative manner. As a first address of this challenge, we compare here quantitative parameters characterizing intracellular gene delivery steps for an E1/E3-deleted adenoviral vector and three polyethylenimine (PEI)-based vector formulations, as well as the liposomal transfection reagent Lipofectamine and naked DNA; the cargo is a plasmid encoding the β-galactosidase gene under a CMV promoter, and the cell host is the C3A human hepatocellular carcinoma line. The parameters were determined by applying a previously validated mathematical model to transient time-course measurements of plasmid uptake and trafficking (from whole-cell and isolated nuclei lysates, by real-time quantitative PCR), and gene expression levels, enabling discovery of those for which the adenoviral vector manifested superiority. Parameter-sensitivity analysis permitted identification of processes most critically rate-limiting for each vector. We find that the adenoviral vector advantage in delivery appears to reside partially in its import to the nuclear compartment, but that its vast superiority in transgene expression arises predominantly in our situation from postdelivery events: on the basis of per-nuclear plasmid, expression efficiency from adenovirus is superior by orders of magnitude over the PEI vectors. We find that a chemical modification of a PEI-based vector, which substantially improves its performance, appears to do so by enhancing certain trafficking rate parameters, such as binding and uptake, endosomal escape, and binding to nuclear import machinery, but leaves endosomal escape as a barrier over which transgene delivery could be most sensitively increased further for this polymer.
Gene Therapy (2005) **12**, 1023–1032. doi:10.1038/sj.gt.3302495; Published online 24 March 2005

Keywords: *molecular conjugates; trafficking; mathematical model; liver*

Introduction

Synthetic gene delivery vectors offer potential advantages over viral vectors for systemic administration. Ease of vector production, customization through conjugation of additional enhancement molecules, and vector property optimization make synthetic vectors an attractive option for gene delivery. Unfortunately, the relative inefficiency of transfection for these vectors compared to their viral counterparts remains the largest barrier to synthetic vector development and application. Elucidating how synthetic and viral vectors behave at the intracellular level is therefore instructive for vector improvement and optimization. This understanding can be advanced by application of mathematical models to quantitatively analyze vector delivery capabilities in terms of parameters that characterize the key delivery pathway steps.

Intracellular pathway steps important for successful gene delivery have been reviewed from a quantitative perspective.[1] Based on published literature reports and dedicated transient vector uptake and nuclear accumulation data, a mathematical model has been previously constructed and validated, which permits parameters representing cell binding, internalization, endosomal escape, unpackaging, and nuclear import to be estimated (Figure 1).[2] Application of this model to similar experimental data for any given vector and cell type of interest should enable quantitative elucidation of which steps are rate-limiting for that vector/cell system. Moreover, comparative analyses among vectors should offer insights into ways in which one vector might be

Correspondence: Professor DA Lauffenburger, Biological Engineering Division, Massachusetts Institute of Technology, MIT, Bldg 56, Room 341, Cambridge, MA 02139, USA
[5]These authors contributed equally to this work
Received 14 June 2004; accepted 16 January 2005; published online 24 March 2005

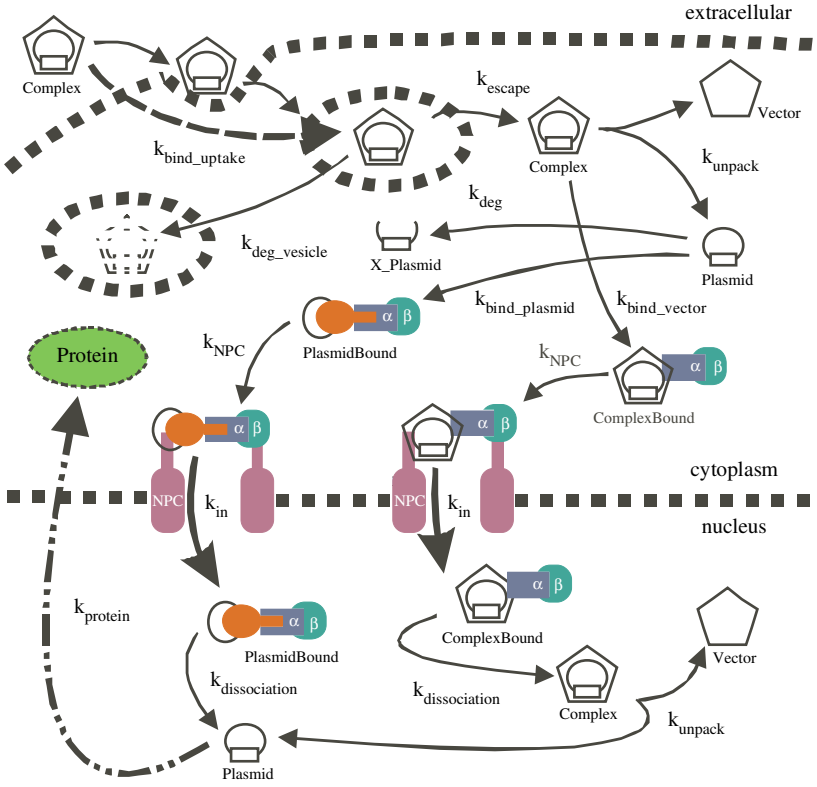

Figure 1 *Schematic diagram of the computational model. Gene delivery begins with the binding and internalization of complexes (k_{bind_uptake}) followed by endosomal escape (k_{escape}) or loss to vesicular degradation ($k_{deg\_vesicle}$). Upon endosomal escape, complexes can be imported into the nucleus (k_{in}) if the cellular nuclear import machinery bind (k_{bind_vector}) and associate with nuclear pores (k_{NPC}). Conversely, the complex may unpackage in the cytoplasm (k_{unpack}), exposing free plasmids and allowing for plasmid nuclear import by a similar mechanism ($k_{bind\_plasmid}$, k_{NPC}, and k_{in}) while plasmid degradation (k_{deg}) simultaneously competes. Within the nucleus, the import machinery dissociates ($k_{dissociation}$), and delivered complexes unpackage (k_{unpack}) to allow for gene expression ($k_{protein}$) (adapted from Varga et al[2]).*

superior or inferior to another at any particular delivery pathway step.

One class of synthetic gene delivery vectors receiving much attention has been that of the polycation polyethylenimine (PEI).[3–11] A branched polymer containing primary, secondary, and tertiary amines, PEI is capable of complexing plasmid DNA and delivering it intracellularly to cells *in vitro*. The amine groups of PEI are thought to act as proton sponges, preventing endosomal acidification, which results in osmotic swelling and disruption of endosomal membranes.[6] This theorized increase in endosomal escape ability has correlated well with the increased gene transfection ability of PEI *in vitro* compared to other polycationic vectors, such as polylysine.[11] To further investigate the influence of cytoplasmic delivery on PEI's efficacy, a novel, N-dodecylated PEI derivative has been prepared. Dodecylation, the addition of a 12-carbon alkyl chain onto PEI, is hypothesized to increase cytoplasmic delivery by raising cellular uptake of PEI by making the polymer more hydrophobic.[9] Recent data in COS-7 cells showed that dodecylation significantly increased cellular uptake of complexes over unmodified PEI,[9] but the intracellular steps responsible for the improvement have not yet been directly ascertained. One aim of our new work here, therefore, is to determine which of the intracellular delivery pathway parameters were most usefully enhanced by this chemical modification strategy.

Moreover, an explicit comparison of PEI vectors to the benchmark of an adenoviral vector in terms of intracellular pathway step parameters has not been undertaken. Hence, a second aim of our work here is to determine which of the delivery pathway parameters are critically superior for the adenoviral vector relative to the PEI vectors.

Both of these aims are addressed by application of our previously validated mathematical model[2] to new data here for delivery of a plasmid encoding the β-galactosidase gene under a CMV promoter to the nuclear compartment of the C3A human hepatocellular line; this is the same plasmid/cell system for which the model was originally validated, so some of the foundational parameter estimates used there are relevant in this new study as well. Here, we measure vector and plasmid accumulation in whole cells and nuclear extracts for the following candidates: an E1/E3-deleted adenoviral vector; three PEI-based formulations – 2 kDa PEI, 25 kDa PEI, and dodecylated 2 kDa PEI; Lipofectamine; and naked DNA. For each of these vector candidates, the following model parameters were determined: the rate constant for cell binding and uptake; the rate constant for intracellular degradation; the rate constant for endosomal escape; the rate constant for binding nuclear import proteins; and the rate constant for unpackaging of the plasmid from the vector. Thus, we are able to directly and quantitatively compare the vectors in terms of their respective values for these various parameter values.

Further, we undertook a quantitative sensitivity analysis to determine for each vector candidate, which parameter remains the most beneficial to enhance in order to improve the transgene delivery process.

Results

Experimental kinetics of transfection

To experimentally examine and compare the kinetics of plasmid internalization and trafficking, various gene delivery vectors were used to deliver a β-galactosidase encoding plasmid into C3A human hepatoblastoma cells: E1/E3-deleted adenovirus, fluorescein-labeled 25 kDa PEI, 2 kDa PEI, N-dodecylated 2 kDa PEI, Lipofectamine, and the no-vector control naked DNA. Cells were transfected at a dose of 5 μg DNA per well for up to 4 h. Periodically, transfection was stopped and the cell samples were aliquoted. PEI uptake was measured for total cellular fractions, followed by total intracellular and nuclear-associated DNA isolation and DNA quantification by real-time PCR. The nuclear-associated fraction consisted of intranuclear and nuclear membrane-bound plasmids. The measured plasmid numbers for total cellular and nuclear-associated fractions were normalized to the endogenous gene for β-actin.

Uptake profiles for 25 kDa PEI and dodecylated 2 kDa PEI were observed to be similar, both exhibiting significantly greater uptake than 2 kDa PEI (Figure 2). Diverse internalization and trafficking kinetics were observed for the various vectors (Figure 3). The PEI-based polymers exhibited the greatest plasmid uptake (total cellular plasmid copies), while Lipofectamine showed the most efficient nuclear trafficking (fraction of nuclear-associated to total cellular plasmid copies) and a more linear profile than the other vectors. Adenovirus also showed efficient nuclear trafficking, but surprisingly delivered substantially less total cellular plasmid than the PEI-based vectors. Indeed, naked DNA provided the same magnitude of total cellular plasmids as the virus, but was largely inadequate in successfully trafficking these plasmids to the nucleus.

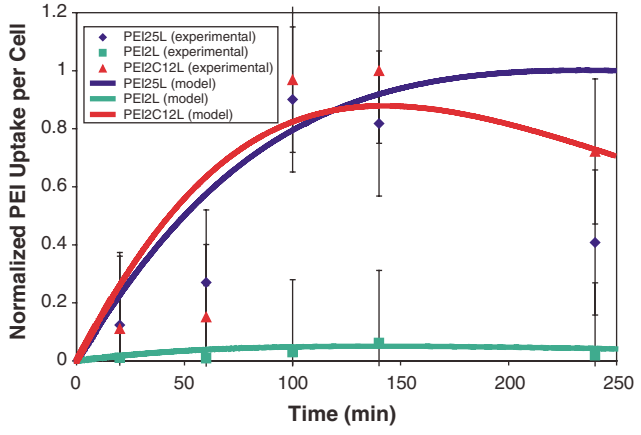

Figure 2 *PEI uptake. Total cellular uptake of fluorescently labeled 25 kDa PEI (PEI25L), 2 kDa PEI (PEI2L), and dodecylated 2 kDa PEI (PEI2C12L) with model fits of total cellular vector copies, obtained from model predictions of transfection. C3A cells were grown to 70% confluence in six-well plates. For each well, 5 μg of DNA was complexed with the appropriate amount of the respective PEI variant to yield an N/P ratio of 20. After addition of the complexes, wells were washed and lysed at the indicated time points. Real-time PCR for the β-actin gene was performed to quantify cell number in a fraction of each sample. Raw fluorescence data were acquired from a fraction of the remaining cell lysate to determine vector uptake for each replicate, and standard dilutions of labeled PEI stocks were run on each plate to determine the concentration of polymer in each sample and verify that each sample was within the linear range of the assay. These values were then normalized on a per cell basis using the corresponding β-actin results. All per cell fluorescence data were then normalized to the maximum per cell fluorescence value observed in the assay, which occurred for PEI2C12L complexes at 140 min.*

Cells transfected by adenovirus yielded the highest gene expression, followed by 25 kDa PEI, Lipofectamine, dodecylated 2 kDa PEI, 2 kDa PEI, and naked DNA, respectively (Figure 4, open bars). Gene expression data were normalized to the 25 kDa PEI value in all cases. Total gene expression for the different vectors varied over five orders of magnitude, with adenovirus outperforming its nearest competitor by nearly two orders of magnitude.

These essentially 'raw' data show interesting phenomena, but by themselves are of limited utility toward the goal of ascertaining which intracellular steps are faster or slower among the various vectors and which is the most critically rate-limiting for any given vector. In order to pursue this quantitative analysis, we turn to application of a mathematical model to determine the key parameters characterizing the intracellular steps for each vector.

Model-based analysis

We have previously constructed and validated a mechanism-based mathematical model for the major potentially rate-limiting intracellular steps involved in gene delivery.[2] The current version of this model is illustrated in Figure 1. Certain parameters in the model retained their previously estimated values, since we are using the same experimental plasmid and cell system as in the earlier validation. These are: the rate constant for degradation of free plasmid in the cytosol, k_{deg}; the rate constant for nuclear import protein binding to plasmids, $k_{bind\_plasmid}$; the rate constant for nuclear pore complex formation, k_{NPC}; the rate constant for translocation into the nuclear compartment, k_{in}; and the rate constant for dissociation of nuclear import protein from plasmid or vector, $k_{dissociation}$. The remaining parameters were determined from the experimental measurements described above, of vector uptake (Figure 2) and plasmid uptake and trafficking (Figure 3). These are the rate constant for binding and uptake of vector/plasmid complexes into the cell, k_{bind_uptake}; the rate constant for plasmid degradation (presumably in the lysosomal compartment), $k_{deg\_vesicle}$; the rate constant for escape of vector/plasmid complexes from the endosomal compartment, k_{escape}; the rate constant for nuclear import protein binding to vectors, k_{bind_vector}; and the vector/plasmid unpackaging rate constant, k_{unpack}. These parameters represent the processes most likely to depend on a particular vector used.

Best-fit model predictions for transient data on vector uptake (Figure 2) and plasmid uptake and trafficking (Figure 3) were obtained by determining the values for the rate constants delineated above (k_{bind_uptake}, k_{escape}, $k_{deg\_vesicle}$, k_{bind_vector}, k_{unpack}), with the other parameters held constant at their previously determined values (k_{deg}, $k_{bind\_plasmid}$, k_{NPC}, k_{in}, $k_{dissociation}$). Mathematically, total

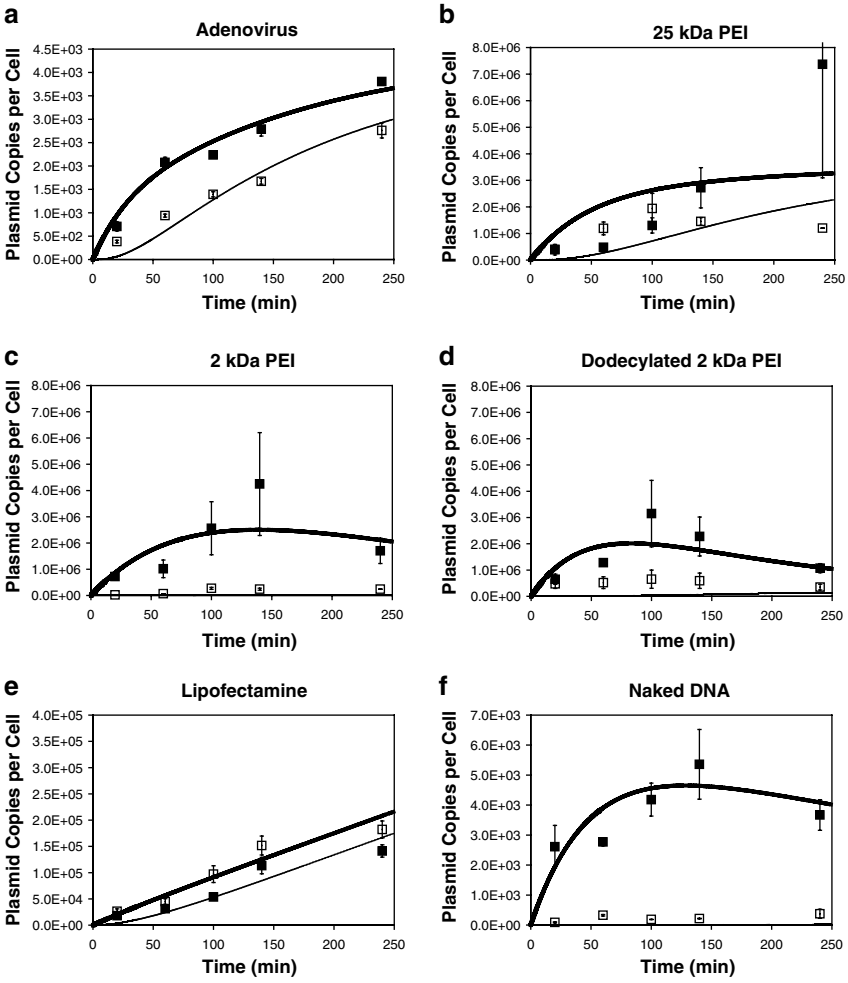

Figure 3 *Experimental kinetic data and model predictions. Results of transfections by (a) adenovirus, (b) 25 kDa PEI, (c) 2 kDa PEI, (d) dodecylated 2 kDa PEI, (e) Lipofectamine, and (f) naked DNA for total cellular samples (filled squares) and nuclear-associated fractions (open squares). All plasmid values are normalized to the β-actin gene. Lines represent model predictions of experimental data where only vector-related parameters (uptake, endosomal escape, vesicular degradation, nuclear import protein to vector binding, and unpackaging) are fit per transfection method. All remaining parameters were held constant across all vector fits.*

cellular plasmids included all nondegraded species within the cell, while the nuclear-associated plasmid numbers included both nuclear membrane-associated and intranuclear species. The model fits yielded free intact intranuclear plasmid copies that correlated well with gene expression data, with the exception of adenovirus (Figure 4, solid bars). Free intact intranuclear plasmid copies were normalized to the 25 kDa PEI copy number.

The vector rate constant values ranged from 0.5 s^{-1} for unpackaging of 2 kDa PEI complexes, to 1×10^{-5} s^{-1} for endosomal escape of naked DNA (Table 1). These extremes of the fit values represent characteristic half-lives of 1.4 s and 19.3 h, respectively. The parameters for unpackaging (k_{unpack}) and binding of nuclear import machinery to vectors (k_{bind_vector}) were not included for naked DNA delivery as there is no vector involved. Also, unpackaging (k_{unpack}) and endosomal escape (k_{escape}) were assumed to be instantaneous and binding of nuclear import machinery to vectors (k_{bind_vector}) not significant for Lipofectamine, as is characteristic of liposomal transfection agents,[2,12,13] and therefore not included. The resulting computational results were consistent with crucial features of the experimental data (Figure 3), with goodness-of-fit R^2 values ranging from 0.58 to 0.99 with an average R^2 value of 0.81 ± 0.14.

Comparison of the various rate constants across the set of vectors shows a number of intriguing results. The adenoviral vector exhibits faster endosomal escape and nuclear import protein binding, though slower plasmid unpackaging, than the PEI vector formulations, and was comparable to these vectors in binding and uptake. Among the PEI vector formulations, the following trends were found: Dodecylated 2 kDa PEI showed a modest increase in binding and uptake over 25 kDa PEI, with 2 kDa PEI being the least efficient at this step. At the same time, this modified PEI showed the fastest vesicular degradation kinetics, doubling the rate of 2 kDa PEI, with the 25 kDa PEI vector once again being intermediate. The 25 kDa PEI displayed superiority in endosomal escape ability over both 2 kDa vectors, but dodecylation did markedly improve this step. Both 25 kDa PEI and dodecylated 2 kDa PEI bind nuclear import proteins significantly better and unpackage more slowly than 2 kDa PEI. Lipofectamine showed substantially slower binding and uptake than all other

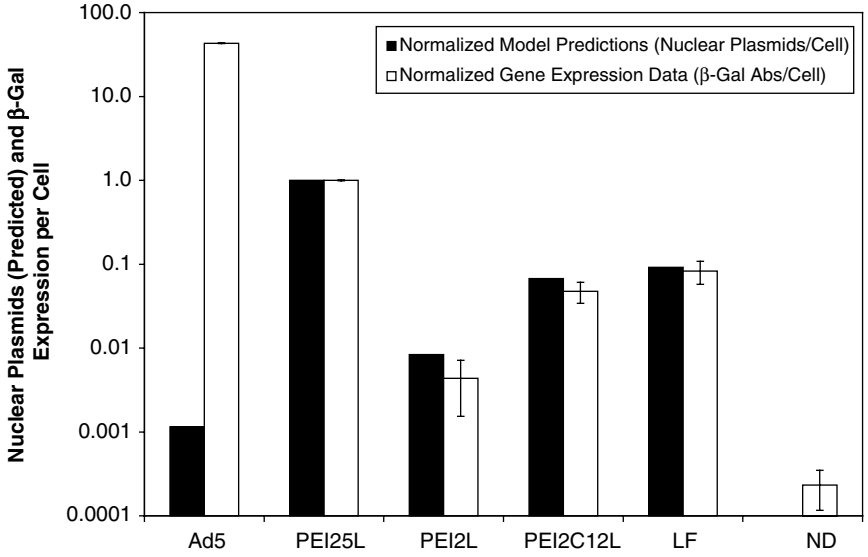

Figure 4 *Gene expression. Normalized per cell expression of the β-galactosidase gene at 48 h post-transfection (open bars) by adenovirus (Ad5), 25 kDa PEI (PEI25L), 2 kDa PEI (PEI2L), dodecylated 2 kDa PEI (PEI2C12L), Lipofectamine (LF), and naked DNA (ND) and normalized free intact nuclear plasmid copies per cell from model predictions (solid bars). Implementation of the mathematical model yielded normalized nuclear plasmids/cell figures, while β-gal absorbance readings (at $\lambda = 420$ nm) were normalized on a per cell basis by performing quantitative, real-time PCR for the β-actin gene for each sample. Values for both nuclear plasmids predicted by the model and experimentally measured β-gal expression for each vector were then normalized to the 25 kDa PEI (PEI25L) values.*

Table 1 Vector rate constant values

	Bind_Uptake	*Deg_Vesicle*	*Escape*	*Bind_Vector*	*Unpack*
Ad5	6.0×10^{-3}	2.0×10^{-2}	1.6×10^{-2}	1.0×10^{-1}	1.0×10^{-2}
PEI25L	6.0×10^{-3}	1.5×10^{-2}	1.0×10^{-2}	4.0×10^{-2}	5.0×10^{-2}
PEI2L	5.0×10^{-3}	1.0×10^{-2}	5.0×10^{-5}	1.0×10^{-5}	5.0×10^{-1}
PEI2C12L	7.0×10^{-3}	2.0×10^{-2}	6.0×10^{-4}	2.0×10^{-2}	8.0×10^{-2}
LF	7.0×10^{-5}	2.0×10^{-2}	—	—	—
ND	2.0×10^{-3}	2.0×10^{-2}	1.0×10^{-5}	—	—

Gene delivery parameter values reported in units of min^{-1} from vector transfections and model predictions by adenovirus (Ad5), 25 kDa PEI (PEI25L), 2 kDa PEI (PEI2L), dodecylated 2 kDa PEI (PEI2C12L), Lipofectamine (LF), and naked DNA (ND) for the vector specific processes of endosomal escape (Escape), nuclear import machinery to vector binding (Bind_Vector), vector unpackaging (Unpack), cellular binding and uptake (Bind_Uptake), and vesicular degradation (Deg_Vesicle), represented by the mathematical model rate constants k_{escape}, k_{bind_vector}, k_{unpack}, k_{bind_uptake}, $k_{deg\_vesicle}$, respectively.

vectors, while naked DNA displayed binding and uptake that was less efficient than the adenovirus and PEI vectors and had the poorest endosomal escape ability, as was expected.

These results thus permit comparison between different vectors, elucidating which steps are faster for a superior vector relative to an inferior vector. That would seem to suggest that enhancing the parameter representing an inferior step should enable improvement of the delivery capability of the less efficient vector. However, if that step is not a significant rate-limiting step for the inferior vector, enhancing it will still not substantially improve the overall delivery capability. Hence, we need to turn to sensitivity analysis to learn about which steps are significantly rate-limiting for any given vector.

Sensitivity analysis

As described in the Materials and methods section, we employed a computational algorithm to generate a sensitivity analysis profile for delivery of intact unpackaged intranuclear plasmids by the various gene delivery vectors investigated (Figure 5). Each value represents the relative sensitivity of intact unpackaged intranuclear plasmids to a change in each model parameter. The larger the sensitivity value, the more effect a change in that particular model parameter would have on obtaining intact unpackaged intranuclear plasmids. Therefore, for each individual vector, the model parameter with the greatest sensitivity represents the rate-limiting process for nuclear delivery of intact unpackaged plasmid. From the sensitivity analysis, the rate-limiting process for adenovirus was nuclear import of plasmid (k_{in}) while cellular uptake (k_{bind_uptake}) was also a sensitive parameter. However, these sensitivities were at least three orders-of-magnitude lower than the highest sensitivity for the other vectors. Nuclear import of plasmid (k_{in}) was also rate-limiting for 25 kDa PEI transfection, with cellular binding and uptake (k_{bind_uptake}) and endosomal

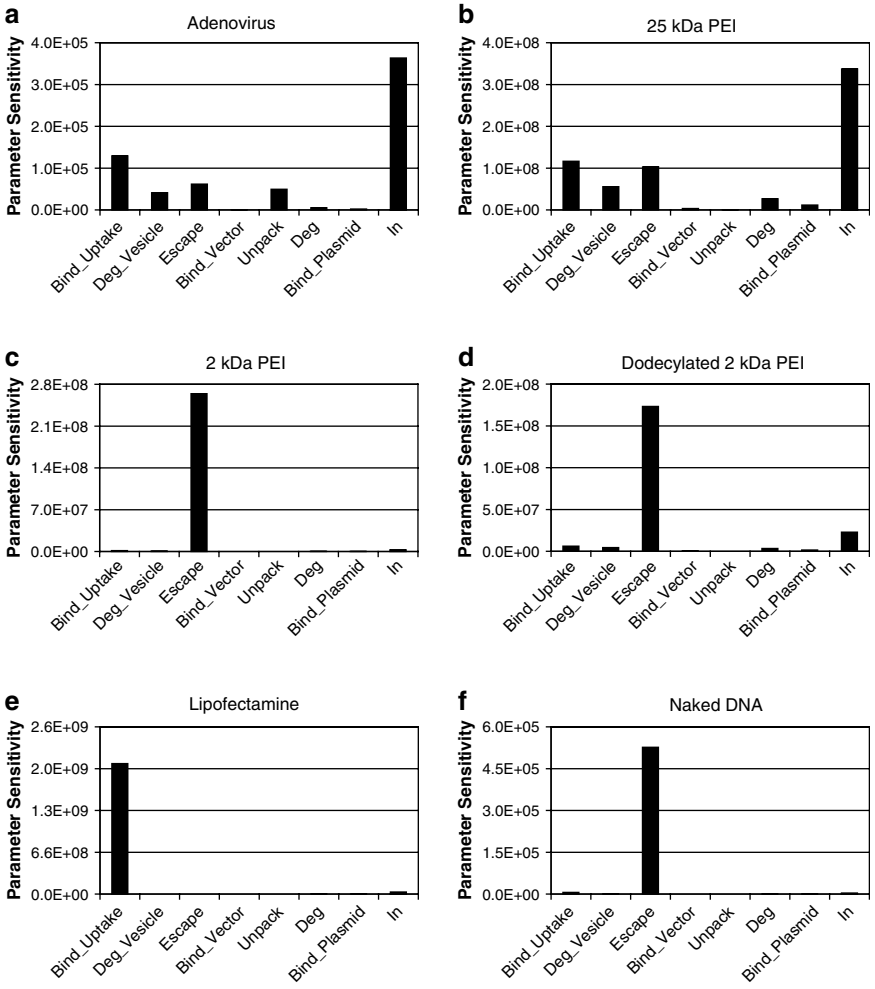

Figure 5 *Sensitivity analysis. Sensitivity of intact free nuclear plasmids delivered by the gene delivery vectors (a) adenovirus, (b) 25 kDa PEI, (c) 2 kDa PEI, (d) dodecylated 2 kDa PEI, (e) Lipofectamine, and (f) naked DNA to various model parameters representing sequential steps in the intracellular gene delivery processes: cellular binding and uptake (Bind_Uptake), vesicular degradation (Deg_Vesicle), endosomal escape (Escape), nuclear import machinery to vector binding (Bind_Vector), vector unpackaging (Unpack), degradation of cytosolic plasmids (Deg), nuclear import machinery to plasmid binding (Bind_Plasmid), and nuclear import (In). Largest sensitivity values represent the rate-limiting process for a particular vector.*

escape (k_{escape}) also sensitive. The model indicated endosomal escape (k_{escape}) as the rate-limiting process for the other PEI vectors and naked DNA with nuclear import of plasmid (k_{in}) being slightly more sensitive for the dodecylated 2 kDa PEI, while Lipofectamine had cellular binding and uptake (k_{bind_uptake}) as the rate-limiting process.

Discussion

Creating synthetic gene delivery vectors with viral-like transfection efficiencies continues to be an important goal in gene therapy research. Current research on vector design is evolving from focus on individual barriers to efficient gene delivery to vector design motivated by a systematic analysis of multiple steps in an integrated manner. As viruses are less easily changed, modified, and developed, the desire to apply these same analyses to virus characterization and development is relatively new. To more completely understand mechanism-based vector development, these novel potential synthetic vectors must be compared to the current 'gold standard' for transfection, viral vectors.

One nonviral vector in particular, PEI, has emerged as a promising candidate in synthetic vector development. In our current study, therefore, cells were transfected with a β-galactosidase expressing plasmid via 25 kDa PEI, 2 kDa PEI, and dodecylated 2 kDa PEI as well as by Lipofectamine, adenovirus, and naked DNA to compare the mechanistic delivery processes of a viral vector with both well studied and novel synthetic carriers. As current synthetic gene delivery vector development seeks to create systems capable of achieving near-viral transfection efficiency, observing viral uptake and trafficking kinetics provides information useful for determining the relative features that can be potentially engineered into a synthetic carrier to make it a better delivery agent.

At the cellular and intracellular level, each of the individual steps discussed in Figure 1 can serve as a potentially rate-limiting step to successful gene delivery and expression. Here, this was directly examined experimentally and then analyzed by the mathematical

model to gain added insight into the specific steps that were important for each vector. Combining quantitative experimental measurement with computational modeling has the potential to glean information about a given system, which would be otherwise unattainable or seem counterintuitive if approached along one of these paths alone.

We employed fluorescent labeling of the various PEIs for direct measurement of vector uptake kinetics to test the hypothesis that dodecylation would also increase cellular uptake in this experimental system and that increased uptake would correlate with gene expression levels for all PEI vectors. The 25 kDa PEI (PEI25L) and dodecylated 2 kDa PEI (PEI2C12L) showed similar uptake kinetics, both significantly over that of the 2 kDa PEI (PEI2L) (Figure 2, data points), supporting the notion of increased uptake by dodecylation and providing a first indication for 2 kDa PEI's lower efficiency as a gene delivery agent. It is generally known that 2 kDa PEI forms larger particles than its higher MW variants, which was substantiated by our sizing studies (see Materials and methods), and can have the tendency to aggregate during transfection,[14,15] hindering endocytosis and possibly explaining the diminished uptake that was observed.

To obtain the experimental transient time profiles for plasmid uptake and trafficking kinetics requisite for our mathematical model-based analysis, we used a nuclear isolation protocol, DNA purification, and real-time PCR. We found that each vector demonstrated unique uptake and nuclear trafficking kinetics (Figure 3). While the PEI-based gene delivery vector transfections (Figure 3b–d) exhibited the greatest total cellular plasmid uptake, Lipofectamine (Figure 3e) had the most efficient nuclear trafficking kinetics (ratio of nuclear-associated to total cellular plasmids), and the most linear profile, possibly due to a delivery mechanism that involves fewer total cellular compartments. Transfection by adenovirus (Figure 3a) yielded the lowest plasmid uptake, but was extremely efficient, internalizing almost 50% of the plaque-forming unit measurement of dose by 4 h. In addition to cellular uptake, adenoviral nuclear trafficking was highly efficient. Naked DNA plasmid uptake occurred with intermediate efficiency but had poor nuclear trafficking (Figure 3f), due in part to its inability to efficiently escape endosomes and its greater susceptibility to degradation inside the cell.

The mass-action model previously constructed[2] was employed to dissect the vector and plasmid uptake and trafficking data and investigate the possible mechanistic differences in vector performances. A modified version of the published mathematical model was used where complex vesicular degradation was included, $k_{deg\_vesicle}$, as well as the separation of nuclear import protein association of vectors and plasmids, k_{bind_vector} and $k_{bind\_plasmid}$, respectively (Figure 1). The processes of vesicular degradation were included to contribute to plasmid and vector loss during transfection (Figures 2 and 3). Nuclear import protein association kinetics were separated for vector and plasmid to capture nuclear uptake behavior observed for various vectors previously[11,16] while maintaining the vector-independent characteristics of plasmid import within C3A cells.

To perform model predictions of the experimental data, only vector-specific parameters were varied for each transfection, while the remaining cellular and plasmid parameters were maintained constant. The resulting predictions followed trends within the experimental data for vector uptake kinetics (Figure 2) and both total cellular and nuclear-associated fractions (Figure 3). Model fits also yielded free intact intranuclear plasmid copies that correlated well with gene expression, with the exception of adenovirus, whose gene expression dramatically exceeded that expected from nuclear plasmid copy numbers relative to those obtained for the synthetic vectors (Figure 4). This in itself presents an exciting and interesting phenomenon, discussed in more detail below.

Fit values of vector rate constant parameters varied over six orders of magnitude, representing a wide range of relatively fast processes, such as 2 kDa PEI unpackaging, to slow processes, such as endosomal escape of naked DNA (Table 1). These data alone offer qualitative insight into potential opportunities for vector redesign under the assumption that the slowest process is the rate-limiting step.

To quantitatively investigate and identify rate-limiting processes for transfection by these vectors in C3A cells, a sensitivity analysis was performed (Figure 5). The rate-limiting processes were identified as the model parameters most influential in obtaining free, nondegraded, intranuclear plasmids. For naked DNA, endosomal escape was revealed as the rate-limiting process, consistent with k_{escape} as the smallest kinetic rate constant. For Lipofectamine, cellular uptake (k_{uptake}) was rate-limiting, also the smallest rate constant in magnitude. Endosomal escape was rate-limiting for dodecylated 2 kDa PEI, reflecting that although the polymer was internalized readily, it was inefficiently released into the cytoplasm from endosomes. This could be potentially due to the fact that dodecylation takes up protonation sites on the PEI molecule and may lead to a diminished 'proton sponge' effect when compared to unmodified PEI. The 25 kDa PEI, like dodecylated 2 kDa PEI, was efficient at cellular uptake (Figure 2), yet had increased endosomal escape capabilities, resulting in nuclear import (k_{in}) as the rate-limiting process. Of the polymers tested, 2 kDa PEI was internalized the most inefficiently (Figure 2). While binding of nuclear import machinery to the 2 kDa PEI was the slowest process, endosomal escape was revealed by the sensitivity analysis to be rate-limiting. When parallel pathways exist for plasmid delivery, such discrepancies between the slowest and the most rate-limiting processes can emerge. Here, because 2 kDa PEI unpackages so readily, achieving increased cytoplasmic complexes will be sufficient to achieve increased nuclear plasmid numbers. While facilitating nuclear import of complexes by increasing the slowest process of import machinery binding will result in more intranuclear plasmids, this effect will be less efficient than if more complexes are delivered to the cytoplasm.

Adenovirus was so efficient at achieving delivery of intranuclear, unpackaged, intact plasmids that no parameter emerged as glaringly sensitive (Figure 5). Closer inspection of sensitivity values revealed nuclear import as the rate-limiting process, albeit only incrementally so over endosomal escape, cellular uptake, vesicular degradation, and unpackaging. The efficacy of adenovirus transfection cannot simply be related to any single fast

process, as the vector specific parameter values for adenovirus are comparable to those of the various nonviral vectors. In some cases the rate constants were faster, such as for binding of nuclear import machinery to the vector (Bind_Vector) and endosomal escape (Escape), while other parameters, such as unpackaging (Unpack) and cellular uptake (Uptake) were slower than some (all for unpackaging) of the nonviral vectors (Table 1). Yet the overall combined parameter value matrix of adenovirus resulted in superior vector performance over the nonviral vectors tested. These data further support the requirement for systems level analysis of gene delivery mechanisms; focus on any single process within the gene delivery pathway will not be sufficient to develop vectors with maximal efficacy.

These data clearly reveal the highly evolved efficiency of adenovirus delivery of transgenes. Theoretically, any viral change resulting in a high dependence on a single process would be selected out for during evolution. Even more striking than the plasmid uptake and trafficking data are the gene expression results observed for adenovirus. Gene delivery by adenovirus yielded approximately three orders of magnitude fewer nuclear copies of plasmid, but two orders of magnitude more gene expression, compared to the 25 kDa PEI. Thus, beyond efficient nuclear delivery of plasmid, other factors can contribute significantly to successful gene delivery. Possible mechanistic explanations for the increased gene expression by adenovirus include prolonged gene expression due to decreased gene silencing by methylation, as increases in methylation have been correlated with decreased gene expression.[17,18] While both adenovirus and plasmid consisted of the β-galactosidase gene under a CMV promoter, the sequences were not identical, and thus promoter strength could contribute to the differences in gene expression.

Another possibility for the difference in gene expression can be related to the observed slowed unpackaging for adenovirus compared to the synthetic vectors (lower k_{unpack} parameter value, Table 1). Potential facilitation of transcription factor recruitment by the still associated viral proteins, similar to the observed facilitation of nuclear import protein binding (higher $k_{\text{bind\_vector}}$ parameter value, Table 1) could beneficially influence gene expression of the virus, an aspect not captured in the mathematical model. It is unlikely the synthetic vectors were able to recruit transcription factors such that unpackaging, while protecting plasmid from cytoplasmic nucleases, could only be detrimental upon intranuclear delivery. Adenoviral terminal protein may contribute to this transcription factor recruitment, plasmid presentation, and gene expression. This viral protein is involved in binding to the nuclear matrix and association of transcriptional initiators to the genome.[19,20] Future development of the experimental methods and mathematical models should seek to explore this significant difference between virus and synthetic vectors.

Further, the additional sequences within the adenoviral genome may similarly increase recruitment of transcription factors and result in the increased gene expression observed. The adenovirus genome contains additional promoters and enhancers for the various viral genes in addition to the CMV promoter for the β-galactosidase gene. These additional elements may contribute to recruitment of transcription factors and expression of the reporter gene.

These potential mechanisms, as well as others, most likely combine in a synergistic manner to enhance gene expression. Such results reinforce the need to optimize not only the gene delivery vector but also the plasmid sequence, to create synthetic therapeutics with the highest possible efficiency. As such, future research should focus on the intracellular events resulting in the enhanced gene expression by adenovirus. Specifically, experimental investigation of the underlying mechanisms and testing model predictions into the possible processes will serve to give insight into a potentially exciting discovery. Therefore, in addition to vector development, other postdelivery aspects may be rate-limiting. This finding requires further experimentation and model analysis of the postnuclear-association processes to fully investigate these data. Use of adenoviral DNA as the free plasmid would be a key step in dissection of possible mechanisms of facilitated gene expression.

Identification of rate-limiting processes guides vector improvement and redesign. Increasing endosomal escape of naked DNA is predicted to increase transfection, and has driven nonviral gene delivery research. Lipofectamine would benefit from increased cellular uptake possibly through centrifugation of complexes to the cell surface. Such facilitation of liposomal gene delivery has been shown to increase gene expression.[21] As the cellular process of nuclear import is not easily manipulated, increasing cellular uptake of adenovirus will increase plasmid delivery. A similar argument can be made for 25 kDa PEI. Addition of targeting ligands to 25 kDa PEI could achieve such facilitation through initiation of receptor-mediated endocytosis, a more efficient method of complex internalization. Sensitivity analysis revealed endosomal escape as rate-limiting for both dodecylated and unmodified 2 kDa PEI.

The foregoing potential improvements for nonviral gene delivery vector development originate from an *in vitro* approach. *In vivo* barriers, such as delivery of complexes directly to tissues or intravenously, blood transport and component interaction, transport to organs, systemic clearance, and diffusion through tissues to cells of interest, while outside the scope of this research, are clearly vital as well to effective therapeutic development.

Materials and methods

TaqMan real-time quantitative PCR

Plasmid quantification was performed using the PE Biosystems Prism 7700 (Applied Biosystems, Foster City, CA, USA). β-Galactosidase plasmid forward and reverse primers and probe were designed using Primer Express Software (Applied Biosystems) and yielded sequences for forward primers, reverse primers, and dual labeled probes. Two sets of forward and reverse primers with probe were ordered and tested for optimal efficacy, as determined by widest spread of linear standard curve range and steepest slope of standard curve (Applied Biosystems). The resulting primers and probe spanned an 80 bp region in the β-gal coding region of the plasmid and had sequences: forward primer (5′-TTA CAG GGC

GGC TTC GTC T-3′), reverse primer (5′-TAA GCC GAC CAC GGG TTG-3′), and dual labeled probe (5′-6FAM-CTG GGT GGA TCA GTC GCT GAT TAA ATA TGA TG-TAMRA-3′), used at concentrations of 400/400/25 nM, respectively. For β-actin amplification and quantitation, forward and reverse primers and probe were purchased as a standard kit from Applied Biosystems. The β-actin amplification spanned 295 bp with sequences: forward primer (5′-TCA CCC ACA CTG TGC CCA TCT ACG A-3′), reverse primer (5′-CAG CGG AAC CGC TCA TTG CCA ATG G-3′) and probe (5′-ATG CCC TCC CCC ATG CCA TCC TGC GT-3′). All PCR cycle conditions were 50°C for 2 min, 95°C for 10 min, followed by 40 cycles of 95°C for 15 s and 60°C for 1 min.

Plasmid, polymers, virus, and cell line

Plasmid gWiz-β-Galactosidase (Gene Therapy Systems, San Diego, CA, USA) encodes the enzyme β-galactosidase controlled by the human cytomegalovirus (CMV) promoter. The plasmid DNA was purchased purified and ready for use from a contract plasmid manufacturing company (Aldevron, Fargo, ND, USA). The adenovirus type 5 with E1 and E3 deletions encoding β-galactosidase under a CMV promoter was purchased from Vector Core (University of Michigan, Ann Arbor, MI, USA).

The 2 and 25 kDa PEIs were purchased from Sigma-Aldrich (St Louis, MO, USA). These two polymers and the dodecylated 2 kDa PEI synthesized and characterized by NMR as described previously[9] were labeled with fluorescein following a modified literature procedure.[22] PEI chain to fluorescein ratio used was 1:1.3, and the concentrated stocks were diluted with PBS to obtain 10 mM PEI monomer working stocks.

Transfections were performed in the C3A hepatoblastoma cell line cultured at 37°C and 5% CO_2 in modified essential medium (MEM) supplemented with 10% fetal bovine serum (FBS) and penicillin/streptomycin (all were from ATCC, Manassas, VA, USA). The HepG2 cell line, the parental cells for C3A hepatocarcinoma cells, is known to express α_v integrins, coreceptors for adenovirus infection.[23] Human liver cells are also believed to express the primary adenovirus receptor, coxsackievirus and adenovirus receptor (CAR).[24] As such, viral binding to C3A is receptor-mediated, compared to the nonspecific fluid-phase uptake for the other vectors.

Cellular binding and uptake assay

Fluorescein-labeled PEI was quantified for total cellular binding and uptake using a 96-well fluorescent microplate reader (Molecular Devices, Sunnyvale, CA, USA). C3A cells were transfected with fluorescein labeled polycation. At designated time points, transfection was stopped, cells rinsed to remove extracellular complexes, trypsinized, and frozen overnight to achieve cell lysis. Total fluorescence of the cell lysate was measured with excitation of 485 nm and emission of 530 nm. Standard dilutions of labeled PEI stocks were run on each plate to determine the concentration of polymer in each sample.

Transfection, DNA isolation, and expression assay

For transfection, 5×10^5 cells were plated in six-well Corning plates (VWR, Boston, MA, USA) until 70% confluent. Cells were washed once with PBS and media replaced with growth media containing 5 μg/ml aphidicolin (Sigma Chemical Co, St Louis, MO, USA) and incubated overnight to synchronize cells at the G1/S phase transition, ensuring the presence of a nuclear membrane. Complexes were formed by adding the polymer of interest at N:P ratio of 20:1 to 5 μg DNA per well, mixed by pipetting, and incubated for 30 min at room temperature, then diluted in serum-free medium containing 5 μg/ml aphidicolin final concentration. Nonviral particle size was ascertained via dynamic light scattering using a ZetaPALS Zeta Potential Analyzer with ZetaPALS Particle Sizing Software Version 2.3 (Brookhaven Instruments Corporation, Holtzville, NY, USA). Number-averaged particle diameters were determined over a lognormal distribution for each PEI vector/plasmid complex. The 25 kDa PEI complexes measured 217.0 ± 49.3 nm in diameter, the 2 kDa PEI complexes were 254.3 ± 64.2 nm, and the dodecylated 2 kDa PEI complexes were more compact at 139.7 ± 17.8 nm. Lipofectamine (Gibco BRL, Rockville, MD, USA) complexes were formed at a ratio of 30 μl Lipofectamine to 5 μg DNA per well. Adenovirus was used at 5 μg viral DNA per well, which corresponded to 1.3×10^{11} viral particles, or an MOI of approximately 10^4 PFU/cell. Complexes were prepared in duplicate.

Cells were washed with PBS containing 5 μg/ml aphidicolin, aspirated, then transfected with 1 ml of transfection solution per well for increasing durations, 3 wells per complex per time point, in duplicate. At each time point, transfection was interrupted with extracellular plasmids diluted and removed by double 4°C PBS washes to inhibit internalization and intracellular trafficking, followed by cellular trypsinization with 0.325 ml of trypsin (Sigma) per well. Cells from triplicate complex preparations were combined for nuclear isolation, and 200 μl of the pooled sample was removed for polymer uptake assay and total cellular DNA isolation. Nuclear samples were subjected to centrifugation at 600 *g* for 5 min at 4°C. Nuclear isolation followed a modified standard protocol whereby 0.5% (v/v) NP-40 in a buffer supplemented with 10 mM TrisCl, pH 7.4, and 3 mM $MgCl_2$ was used to achieve cell lysis; the nuclear pellet was centrifuged to remove the supernatant containing cytosolic plasmids and cellular debris. Nuclear fractions were estimated to be $\geqslant$95% pure, as no whole cells were visible among the intact nuclei after lysis, but a small volume of residual cytoplasmic supernatant remained after its removal from the nuclear pellet.

Fluorescein-labeled PEI total cellular samples were quantified for polymer uptake using the uptake assay. DNA purification followed from purified nuclei or whole cells using the DNeasy 96 Tissue Kit (Qiagen, Valencia, CA, USA).

β-Galactosidase gene expression was measured 2 days post-transfection per manufacturer's protocol (Promega, Fitchburg, WI, USA). Results were expressed as enzyme activity in reactant absorbance per cell, normalized to cell numbers from parallel transfected wells.

Computational model and sensitivity analysis

The mathematical model for intracellular gene delivery was used as previously described (Figure 1).[2] As can be seen in Figure 1, a number of sequential and parallel steps have been characterized as first-order mass action events. First, binding and uptake of the vector/plasmid complex into the cell endosomal compartment is combined as a single first-order event, with rate constant

k_{bind_uptake}. Next, the degradation of the vector/plasmid complex (likely via trafficking to the lysosomal compartment) is modeled as a first-order event with rate constant $k_{deg\_vesicle}$. In parallel, the vector/plasmid complex can escape from the endosomal compartment, as a first-order step with rate constant k_{escape}. Cytosolic complexes can bind nuclear import protein with rate constant k_{bind_vector}, or unpackage into vector and plasmid with rate constant k_{unpack}. Unpackaged plasmid can bind nuclear import protein with rate constant $k_{bind\_plasmid}$, or alternatively can be degraded in the cytosol via first-order kinetics with rate constant k_{deg} before this binding occurs. Translocation of nuclear import protein-bound vector or plasmid into the nuclear compartment is modeled to occur in first-order manner with rate constant k_{in}, after formation of a nuclear pore complex described by rate constant k_{NPC}. Once in the nuclear compartment, vector/plasmid complex can unpackage into vector and plasmid with rate constant k_{unpack}, as in the cytosol. Complexes and plasmid bound to nuclear import protein can dissociate that protein, with rate constant $k_{dissociation}$. Finally, gene expression can be modeled with the lumped, first-order rate constant $k_{protein}$.

The following parameters retained their previously estimated values: $k_{bind\_plasmid}$, k_{deg}, k_{NPC}, k_{in}, and $k_{dissociation}$.[2] The remaining parameters (k_{bind_uptake}, k_{escape}, $k_{deg\_vesicle}$, k_{bind_vector}, and k_{unpack}) were determined from the experimental measurements accomplished herein, of vector uptake (Figure 2) and plasmid uptake and trafficking (Figure 3). Model predictions and parameter fits were performed using Abacuss II software (MIT, Cambridge, MA, USA). Fit parameters were varied until goodness-of-fits were maximized. Imbedded into the modeling software is the capability to perform sensitivity analyses. The modeling program performs the differentials required to generate sensitivity data for each species and parameter internally and therefore parameters need not be varied externally to generate sensitivity data. Further, the resulting sensitivity data represent instantaneous sensitivities, not sensitivity estimates generated by the latter method. Both model and sensitivity results for each given parameter set were imported into Excel (Microsoft Corp., Redmond, WA, USA) and plotted.

Acknowledgements

This work was supported by the NSF Biotechnology Process Engineering Center at MIT. We are grateful to Dr Thomas Wickham for very helpful comments and suggestions.

References

1 Varga CM, Wickham TJ, Lauffenburger DA. Receptor-mediated targeting of gene delivery vectors: insights from molecular mechanisms for improved vehicle design. *Biotechnol Bioeng* 2000; **70**: 593–605.
2 Varga CM, Hong K, Lauffenburger DA. Quantitative analysis of synthetic gene delivery vector design properties. *Mol Ther* 2001; **4**: 438–446.
3 Akinc A, Langer R. Measuring the pH environment of DNA delivered using nonviral vectors: implications for lysosomal trafficking. *Biotechnol Bioeng* 2002; **78**: 503–508.
4 Forrest ML, Pack DW. On the kinetics of polyplex endocytic trafficking: implications for gene delivery vector design. *Mol Ther* 2002; **6**: 57–66.
5 Abdallah B *et al*. A powerful nonviral vector for *in vivo* gene transfer into the adult mammalian brain: polyethylenimine. *Hum Gene Ther* 1996; **7**: 1947–1954.
6 Boussif O *et al*. A versatile vector for gene and oligonucleotide transfer into cells in culture and *in vivo*: polyethylenimine. *Proc Natl Acad Sci USA* 1995; **92**: 7297–7301.
7 von Harpe A, Petersen H, Li Y, Kissel T. Characterization of commercially available and synthesized polyethylenimines for gene delivery. *J Control Release* 2000; **69**: 309–322.
8 Zanta M-A, Boussif O, Adib A, Behr J-P. *In vitro* gene delivery to hepatocytes with galactosylated polyethylenimine. *Bioconj Chem* 1997; **8**: 839–844.
9 Thomas M, Klibanov AM. Enhancing polyethylenimine's delivery of plasmid DNA into mammalian cells. *Proc Natl Acad Sci USA* 2002; **99**: 14640–14645.
10 Godbey WT *et al*. Poly(ethylenimine)-mediated transfection: a new paradigm for gene delivery. *J Biomed Mater Res* 2000; **51**: 321–328.
11 Lynn DM, Anderson DG, Putnam D, Langer R. Accelerated discovery of synthetic transfection vectors: parallel synthesis and screening of a degradable polymer library. *J Am Chem Soc* 2001; **123**: 8155–8156.
12 Zelphati O, Szoka F. Mechanism of oligonucleotide release from cationic liposomes. *Proc Natl Acad Sci USA* 1996; **93**: 11493–11498.
13 Lappalainen K *et al*. Intracellular distribution of oligonucleotides delivered by cationic liposomes: light and electron microscopic study. *J Histochem Cytochem* 1997; **45**: 265–274.
14 Godbey W, Wu K, Mikos A. Size matters: molecular weight affects the efficiency of polyethylenimine) as a gene delivery vehicle. *J Biomed Mater Res* 1999; **45**: 268–275.
15 Kunath K *et al*. Low-molecular-weight polyethylenimine as a non-viral vector for DNA delivery: comparison of physicochemical properties, transfection efficiency and *in vivo* distribution with high-molecular-weight polyethylenimine. *J Control Release* 2003; **89**: 113–125.
16 Schaffer DV, Fidelman NA, Dan N, Lauffenburger DA. Vector unpacking as a potential barrier for receptor-mediated polyplex gene delivery. *Biotechnol Bioeng* 2000; **67**: 598–606.
17 Hong K, Sherley J, Lauffenburger D. Methylation of episomal plasmids as a barrier to transient gene expression via a synthetic delivery vector. *Biomol Eng* 2001; **18**: 185–192.
18 Verma M. Viral genes and methylation. *Ann NY Acad Sci* 2003; **983**: 170–180.
19 Fredman JN, Engler JA. Adenovirus precursor to terminal protein interacts with the nuclear matrix *in vivo* and *in vitro*. *J Virol* 1993; **67**: 3384–3395.
20 Webster A *et al*. Role of preterminal protein processing in adenovirus replication. *J Virol* 1997; **71**: 6381–6389.
21 Verma RS, Giannola D, Shlomchik W, Emerson SG. Increased efficiency of liposome-mediated transfection by volume reduction and centrifugation. *Biotechniques* 1998; **25**: 46–49.
22 Godbey WT, Wu KK, Mikos AG. Tracking the intracellular path of poly(ethylenimine)/DNA complexes for gene delivery. *Proc Natl Acad Sci USA* 1999; **96**: 5177–5181.
23 Nejjari M *et al*. Expression, regulation, and function of alphaV integrins in hepatocellular carcinoma: an *in vivo* and *in vitro* study. *Hepatology* 2002; **36**: 418–426.
24 Bergelson JM. Receptors mediating adenovirus attachment and internalization. *Biochem Pharmacol* 1999; **57**: 975–979.